J. Electrical Systems 20-11s (2024): 1965-1979

Jayshree Dasharath Pawar[1]
Mangesh D. Nikose[2]

Control of Torque Ripple and Rotor Position for SRM (8/6- 4 Phases) Using an Optimization Based Model Predictive Torque Control (MPTC)

Journal of Electrical Systems

Abstract
Switched Reluctance Motor (SRM) is used in most of Electric vehicles and wind energy system. But it has some disadvantages are high torque ripple because of its power supply mode and multiphase communication. In this paper Model Predictive Torque Control (MPTC) with Sailfish Optimization (SFO) is reduce the torque ripple of SRM using Torque Sharing Function (TSF). First, based on flux-linkage characteristic curves acquired from the locked rotor test, an accurate SRM model is created, it predict future operation of SRM drive system. Second, the SFO algorithm is used to optimize TSF parameters for minimize the torque value of SRM. Also developed TSF based MPTC method, which avoids the problem of frequency conversion caused by torque controller. Then Atom Search Optimization (ASO) is used to optimize the position sensor for correct rotor position of the SRM. To verify the MPTC-SFO method is compared with Direct Instantaneous Torque Control (DITC). Both simulation on a four phase 8/6 pole SRM for reduce the torque ripple and select the rotor position. The proposed MPTC-SFO method is higher efficiency than DITC. The obtain result is achieved 19.5 % of torque ripple for the proposed method.

Keywords*: Torque ripple, Rotor position, SRM, TSF, Predictive model, MPTC, ASO, SFO, Flux linkage.*

1. Introduction

The Switched Reluctance Motor (SRM) is an electric motor that runs by reluctance torque, and it is a good conventional drives in some specific application [1]. It is used in Electric vehicles and Wind energy system because of its simple and uneven construction, insensitivity to high temperature, fault tolerance, and high speed operation ability [2, 3]. The main drawback of this motor is large torque ripple because of its multiphase communication and power supply mode, which regulates its application [4]. Nowadays many researches have proposed so many techniques to decrease torque ripple. These techniques can be divided into two set of control, namely Indirect Torque Control (ITC), and Direct Torque Control (DTC) [5, 6]. In ITC, they distributes total torque to each phase through the Torque Sharing Function (TSF), and DTC is reduce the inherent output torque in the SRM [7].

TSF is an efficient torque ripple minimization is used to drives in medium and low speed ranges for SRM. TSFs are optimized and evaluated to the primary objective of low torque ripple, based on four common functions namely cubic, linear, exponential and sinusoidal [8, 9]. Direct Instantaneous Torque Control (DITC) is a developed method to solve the torque ripple problems and it provides fast response to the torque changes [10]. Direct Torque and Flux Control (DTFC) used to control the torque and flux of the SRM. The rotor is the movable part of the SRM, and the rotor position is another main problem in the motor [11, 12]. The position sensor is used to locate the rotor position in SRM, and it generates the computation information for the power converter [13]. The rotor position sensor is used to measure the angular position of the rotor shaft in synchronous electric motors [14].

Model predictive control (MPC), a revolutionary nonlinear system control strategy that uses a predict model to determine the value of the motor's subsequent sampling time, has recently gained popularity [15, 16]. The capability of phase current tracking is improved by a model predictive current control [17]. In summary, the MPC has a set control frequency in addition to avoiding complicated commutation rules [18]. The benefit of the MPC is that it is a multivariable controller that simultaneously controls the outputs while accounting for all of the interactions between the systems variables [19, 20]. In this paper we proposed Model predictive Torque control (MPTC) based Sailfish Optimization (SFO) using TSF strategy has been developed, it is used to derivate the value of next sampling time of the motor. It has fast torque response and also it is more apt for applications of high torque response performance. The ASO algorithm is used to optimize the rotor position of the SRM.

The major objectives of this paper is as follows,

- ❖ Model an optimization based MPTC controller for controlling the torque in the SRM motor.
- ❖ The ASO algorithm for optimize the rotor position of the SRM.
- ❖ Reduce the Torque ripple and select the rotor position of the SRM achieving proper result.

Organization Remainder of this paper is organized as follows, in section 2 the researches for minimizing the torque ripple in the SRM is discussed. In section 3 the proposed method is explained in detail figures. In section 4 discuss the obtained results and section 5 concluded the paper.

[*1]Department of Electrical Engineering, School of Engineering and Technology, Sandip University, Nashik, Maharashtra 422213 India.
[2]Head of Electrical and Electronics Engineering Department, School of Engineering & Technology, Sandip University, Maharashtra 422213, India. *Email: pawar.jayshree.dasharath@gmail.com, hodelectrical@sandipuniversity.edu.in

2. Related works

Ren et al. [21] developed a Model Predictive Control (MPC) based Torque Sharing Function (TSF) was used to reduce the torque ripple in SRM. They established flux linkage characteristics curves from the locked rotor test and predict the future operation state of the SRM system. To reduce the torque ripple in commutation region by using TSF and the TSF is optimized by the Genetic Algorithm (GA). A sector division scheme was developed for to decrease the voltage states of the controller. Then the developed method was reduce the torque and stator copper losses and more efficiency to compare with DITC.

Kimpara et al. [22] have developed Field Reconstruction Method (FRM) based on Non Derivative Optimization (NDO) for mitigate the torque ripple. It leads to higher radial vibration and it was mitigated by adaptive hysteresis band controller. The system simulation and system modelling was initially presented the theoretical basis for this method. They used 8/6 SRM for experimentation, and it was reduce the torque pulsation and aural noise in SRM and prevalent use of SRM in a large range of application.

Al-Amyal et al. [23] have introduced Ant Colony Optimization (ACO) was used to**,** improving the motor efficiency, reduce the torque ripple in the SRM. The multi objective function was created for maximize the torque quality of the machines. The improved Direct Instantaneous Torque Control (DITC) drive is implemented using the best results from this optimization challenge. An effective hysteresis torque controller is also implemented using a novel switching technique. An asymmetric half bridge converters switching mode selection is purely based on the SRM inductance profile.

Chenchireddy et al. [24] have developed Artificial Neural Network (ANN) based to reduce the torque ripple in the SRM. The motor needs a power electronic converter for regulating stator poles. Performance of SRM in comparison to ANN and Hysteresis Current Controller (HCC). The optimum performance for motor starting and running conditions is achieved by ANN based SRM. Reducing starting torque, minimising torque ripple, and lowering starting current and running current are the key outcomes of this research.

Jing et al. [25] developed a Fuzzy Indirect Instant Torque Control (IITC) for reduce the torque ripple in the SRM. First, In order to generate a compensation current in accordance with the torque error, a fuzzy controller is first invented. The input factor merge with artificial experience and additionally, taking into account the connection between electromagnetic torque and current, the output factor is suitably created using the linearized inductance derivative. They used 12/8 three phase SRM for provide the result of torque ripple suppression.

Chen et al. [26] examined based on Torque Sharing Function (TSF) two control methods for torque ripple mitigation in SRM. First control was converts compensation torque into the compensation current through from current look up to reduce current ripple. The alternative is the direct instantaneous torque control technique which substitutes a torque loop for the current loop to more accurately follow the reference torque and lesson torque ripple. The multiple parameters of the identified SRM model obstruct the promotion and application of this developed method control strategy, this could be resolved in the future by decreasing the Fourier functions order and combining it with some changes to the control algorithms for the speed and torque loops.

3. Proposed Methodology

The proposed method is used to reduce the torque and also enhance the system efficiency in the Switched Reluctance Motor (SRM). The main problem of SRM is large torque ripple and rotor position because of its multiphase communication, power supply mode. For reduce the torque ripple, the Model Predictive Torque Control (MPTC) along with Sail Fish Optimization (SFO) is used in the proposed model. The SFO is a population based metaheuristic algorithm. In this algorithm, it is assumed that the sailfish are candidate solutions and the problem's variables are the position of sailfish in the search space. Accordingly, the population over the solution space is randomly generated. The Atom Search Optimization (ASO) is used for selecting the optimal rotor position. This optimization will enhance an efficiency in the SRM. In ASO the position of each atom within the search space represents a solution measured by its mass, with a better solution indicating a heavier mass and vice versa. The proposed MPTC method effectively reduces the torque ripple, improves the torque–ampere ratio and system efficiency, and improves dynamic response. The speed, torque position of the rotor, voltage and current across the stator is analyzed in the four phase 8/6 SRM. The block diagram of proposed method is shown in figure 1.

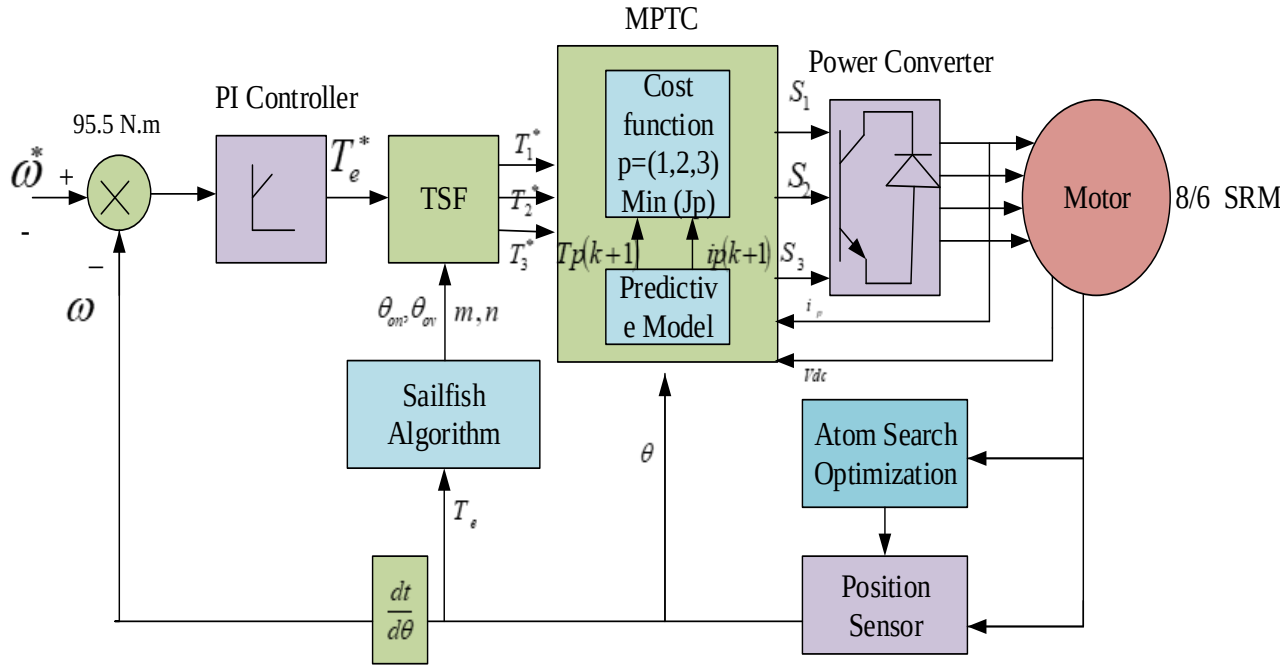

Figure 1: Block Diagram of Proposed SFO-MPTC based SRM

The total value of torque T_e^* is get from PI controller, the value of individual phase torque $T_p^*(p=1,2,3)$ is evaluated by TSF to track current value $ip(k+1)$ and reference toque value $T_p(k+1)$ are predicted in the predictive model. Power converter has 4 voltage states in each phase of the SRM, there are $Sp(1,0,-1)$ and Jp corresponding to 3 voltage states are calculated for each phase winding. $Jp(\min)$ denotes value of minimum predictive, it will select as the optimal voltage state for the next sampling period.

3.1 Torque Sharing Function (TSF)

In communication region, the linear TSF will decrease the torque ripple, and it is consists two stages with $\theta_{on}+0.5\theta_{ov}$ as the midpoint. They defined as,

$$T_p^*=\begin{cases} 0 & (0\le\theta<\theta_{on}) \\ T_e^*\left(\dfrac{2^{m-1}}{\theta^m}(\theta-\theta_{on})^m\right) & (\theta_{on}\le\theta<\theta_{on}+0.5_{ov}) \\ -T_e\left(\dfrac{2^{n-1}}{\theta_{ov}^n}(\theta_{on}+\theta_{ov}-\theta)^n\right)+T_e^* & (\theta_{on}+0.5\theta_{ov}\le\theta<\theta_{on}+\theta_{ov}) \\ T_e^* & (\theta_{on}+\theta_{ov}\le\theta<\theta_{off}) \\ -T_e^*\left(\dfrac{2^{m-1}}{\theta_{ov}^m}(\theta-\theta_{off})^m\right)+T_e^* & (\theta_{off}\le\theta<\theta_{off}+0.5\theta_{ov}) \\ T_e^*\left(\dfrac{2^{n-1}}{\theta_{ov}^n}(\theta_{off}+\theta_{ov}-\theta)^n\right) & (\theta_{off}+0.5\theta_{ov}\le\theta<\theta_{off}+\theta_{ov}) \\ 0 & (\theta_{off}+\theta_{ov}\le\theta<\theta_e) \end{cases} \quad (1)$$

Where, θ_{on} is turn on angle, θ_{off} is turn off angle, θ_{ov} is overlap angle, T_e^* reference torque value. $\theta_e=2\pi/Nr$ Is electrical angle period, Nr is number of rotor poles, m,n are nonlinear TSF curves.

3.1.1 Parameter Optimization based on SFO

SFO algorithm is take to obtain optimal $\theta_{off},\theta_{on},m,n$ .To optimize segmented TSF, taking torque ripple coefficient (T_{ripple}). The function of optimization as,

$$T_{ripple} = \frac{T_{\max} - T_{\min}}{T_{av}} \times 100\% \quad (2)$$

Where $T_{\max}$ are maximum toque value, $T_{\min}$ are minimum torque value, T_{av} are average value, and $Ta-ref, Tb-ref, Tc-ref$ are three phase reference torque, these are distributed by traditional linear strategy of TSF, $Ta, Tb, Tc,$ are three phase actual torque and Te is total torque.

3.2 Model of Switched Reluctance Motor (SRM)

The SRM is an electric machine that converts from mechanical power to reluctance torque, and it has 8 rotor and 12 stator poles. Four coils wound on opposite poles and connected in parallel or series consisting number of electrically separated phases or circuits [27]. The torque is generated by the rotor to align with the stator poles, when the current is passed through the one of the stator winding. The bridge converter contains two diodes and two power switches per phase. This converter can support to control of each phase and handle phase overlap. Equivalent circuit for SRM drive is shown in figure 2.

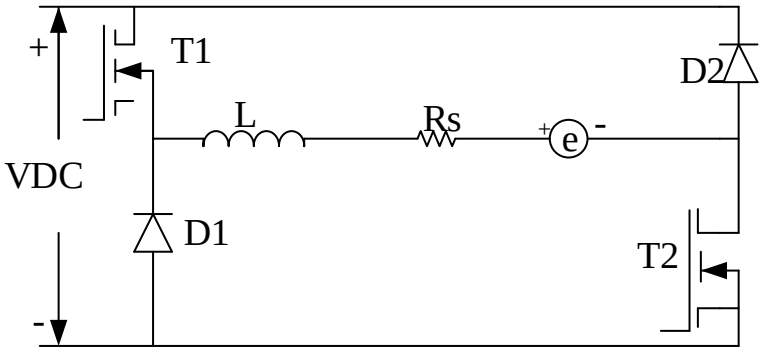

Figure 2: Equivalent Circuit of SRM drive

3.2.1 Torque Equation

The instantaneous voltage across the terminals of one single phase winding for SRM.

$$U_p = i_p R + \frac{d\psi p}{dt} = i_p R + \frac{\partial \psi(i_p, \theta)}{\partial i_p} \cdot \frac{di_p}{d_t} + \frac{\partial \psi(i_p, \theta)}{\partial \theta} \cdot \frac{d\theta}{dt} (P = 1,2,3) \quad (3)$$

Where $U_p, i_p, \psi p, \theta$ are corresponding to the terminals voltage, phase current, winding flux linkage and rotor position. Phase torque equation for SRM

$$T_p = i_p \frac{\partial \psi_p(\theta, i_p)}{\partial \theta} - \frac{\partial W_f}{\partial \theta p} \quad (4)$$

where W_f denotes field energy. The influence of the $\partial W_f / \partial \theta_p$ is very small and can be neglected, due to saturation of the SRM. The instantaneous torque in SRM is

$$T_p \approx i_p \frac{\partial \psi(\theta, i_p)}{\partial \theta} \quad (5)$$

3.2.2. Voltage Equation

According to the basic law of the circuit the voltage equation of the motor for phase j under static stationary reference frame is,

$$U_j = R_j \cdot i_j + \frac{d\psi_j}{dt} (j = 1,2,3) \quad (6)$$

Where, U_j denotes winding voltage, ψ_j denotes winding resistance, i_j denotes winding stator current, R_j denotes winding flux linkage for phase j

To increase the rate of energy conversion, the SRM always operate in the saturation state, resulting in highly nonlinear electromagnetic properties. Therefore, developing a precise nonlinear model of the SRM is a crucial requirement for high performance torque control. There are various ways to create the nonlinear model of SRM, including analytical techniques, neural network techniques and look up table and interpolation techniques.

3.2.3 Establishment of Flux linkage and Torque model

In order to gather reliable flux-linkage data of SRM, the locked rotor test is utilised in this research. The test prototype's rated power is 2.2 kW, and its rated torque is 14 N.m. The flux linkage (ψ) and Torque (T) as expressed following equations,

$$\begin{cases} \psi = Lqi + \left[L_{dsat} i + A\left(1 - e^{-Bi}\right) - Lqi\right] f(\theta) \\ T = \left[\dfrac{(L_{dsat} - Lq)c^2}{2} + \dfrac{A\left(1 - e^{-Bi}\right)}{B}\right] \dfrac{df(\theta)}{dt} \end{cases} \tag{7}$$

$$\begin{cases} A = \psi_m - L_{dsat}\ \mathrm{Im} \\ B = \left(L_d - L_{dsat} / \psi_m - L_{dsat}\ \mathrm{Im}\right) \\ f(\theta) = \left(2N_r^3 / \pi^3\right)\theta^3 - \left(3N_r^2 / \pi^2\right)\theta^2 + 1 \end{cases} \tag{8}$$

Where, L_{dsat} is saturation inductance, ψ_m is flux linkage maximum value, Im is current corresponding to the ψ_m, L_q, L_d denotes the motor inductance of centre line of stator and rotor are completely unaligned and aligned respectively. The flux linkage and torque are functions of rotor position and phase current. Therefore, SRM has torque characteristics and highly nonlinear flux, it makes it's more complicated to control. The flux linkage position and torque position with respect to current is shown in figure 10. Since the SRM's phases are electrically isolated from one another, torque ripple occurs in the commutation regions when the conducting phase is shut off and the ensuing phase is in charge of applying the shaft's reference torque.

3.3. Model Predictive Control (MPC)

MPC has been successfully applied in the process industry and industrial power electronics system. By reduce an objective function at each time step across a finite horizon while being constrained by the models equations, the control action is obtained [29]. The straightforward design is main advantages of MPC, and one just needs to set up an objective function that takes the control objectives into account if they are included in the system model, which should also include restrictions.

3.3.1 Model Predictive Torque Control (MPTC)

MPTC is becoming a powerful control method for SRM drives that require excellent performance control. By directly combined the system model with the finite switching states, MPTC is more efficient and accurate in voltage vector selection as compared to direct torque control [28]. The basic diagram of MPTC is shown in figure 3.

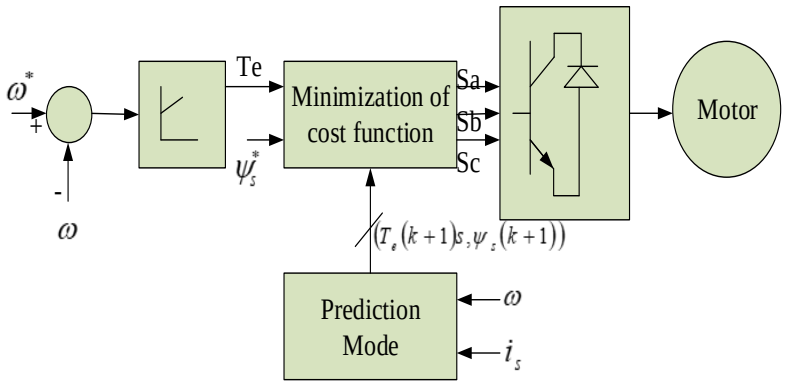

Figure 3: MPTC Basic Diagram

3.3.2 Estimation of stator and rotor flux vectors

In MPTC, it is first necessary to determine the stator flux ψ_s and the rotor flux ψ_r at the current sample time. The stator flux $\hat{\psi}_s(K)$ could be calculated using the Euler formula from the stator voltage in a stationary reference frame as

$$\hat{\psi}_s(K) = \psi_s(k-1) + T_s V_s(k) - R_s T_s i_s(k) \tag{9}$$

The rotor flux $\hat{\psi}_r(k)$ is then estimated in terms of $\hat{\psi}_s(k)$ as

$$\hat{\psi}_r(k) = \frac{L_r}{L_m}\hat{\psi}_s(k) + i_s(k)\left(L_m - \frac{L_r L_s}{L_m}\right) \tag{10}$$

3.3.3 Prediction of Control variables

In MPTC, the stator flux vectors and the electromagnetic torque T_{em} are predicted for the following sampling instant $k+1$. The stator flux vector $\psi_s^p(k+1)$ is predicted using (11) and the Euler formula.

$$\psi_s^p(k+1)=\hat{\psi}_s(K)+T_sV_s(k)-R_sT_si_s(k) \quad (11)$$

The stator voltage vector is expressed as stator flux (9) and rotor current 2 into (10) as,

$$V_s=R_si_s+\left(L_s-\frac{Lm^2}{Lr}\right)\frac{d}{dt}i_s+\frac{Lm}{Lr}\frac{d}{dt}\psi r \quad (12)$$

The rotor flow vector can be calculated from the rotor voltage equation in a stationary reference frame as follows:

$$\frac{d}{dt}\psi_r=\frac{Lm}{\tau_r}i_s-\frac{\psi_r}{\tau_r}+j\omega_r\psi_r \quad (13)$$

Using the Euler formula and the substitution from (9) into (5) the stator current vector prediction is $i_s^p(k+1)$ can be written as

$$i_s^p(k+1)=\frac{T_s}{L_s\sigma}V_s(k)+\left(1-\frac{T_s}{\tau\sigma}i_s(k)+\frac{T_sk_r}{L_s\sigma}\left(\frac{1}{\tau_r}-j\omega_r\right)\hat{\psi}_r(k)\right) \quad (14)$$

Where, $T_\sigma=\frac{L_r\sigma}{R},\sigma=1-\frac{L_m^2}{L_rL_s^2},R_\sigma=R_\sigma+k_r^2R_r and\, k_r^2=\frac{L_m^2}{L_r^2}$ the electromagnetic torque $T^p(k+1)$ could expressed as,

$$T^p(k+1)=\frac{3}{2}\frac{p}{2}I_m\left(\overline{\psi}_s^p(k+1)i_s^p(k+1)\right) \quad (15)$$

Where $\overline{\psi}_s$ is complex conjugate value of the stator flux vector ψ_s

3.3.4 Control Problem

The SRM machines primary goal in control is normally to regulate and maintain its torque close proximity to a reference value, which is typically set by an outer control loop. It include the reducing of the currents and the operation within the rated values, for example, constant phase current below the specified maximum. It is obvious that a motor operated by discrete voltages arbitrarily close to the reference value cannot have its torque regulated at a finite switching frequency. A loss of heat cause by switch transition in the converter, the design of controller is the minimization of the average switching frequency. The control engineer can adjust multiple tuning knobs to balance torque ripple, winding current, and switching frequency by applying varying weights to the control objectives.

The TSF in SRM will be optimized by Sailfish Optimization (SFO) algorithm. SFO simulates the elite population strategy and the alternate sailfish attack on the sardines based on the hunting behaviour of biological groups. Sailfish have greater energy to catch prey early in the hunt, and sardines are also less worn out and damaged. Sardines may so maintain a high rate of escape and have remarkable manipulative skills. Therefore, SFO optimize TSF effectively and identify the torque from particular phase in the TSF with greater energy.

3.4 Sail Fish Optimization (SFO)

Various algorithms and numerous applications could not solve all the optimization problems. The SFO algorithm is metaheuristic algorithm and reduce the method of the group of hunting sailfish. This algorithm makes the assumption that the sailfish are potential solutions and that the variables in the issue are the sailfish's positions in the search space. As a result, the population in the solution space is produced at random [30]. The population of SFO algorithm cover two types, one is the population of sailfish for intensification of the search space, and another one is the population of sardines for diversification of the search space. To derive the algorithm, it is presume that the position of sailfish are the variables of all solutions while the ith member at the kth search agent as a current position $SF_{i,k}$ in a d dimensional search space. The sailfish fitness and sardines computed and the sailfish position will updated at each iteration during the optimization as follows,

$$X^i_{new\_SF}=X^i_{elite\_SF}-\lambda_i\times\left(rand(0,1)\times\left(\frac{X^i_{eliteSF}+x^i_{injured\_s}}{2}\right)-X^i_{oldSF}\right) \quad (16)$$

Where, $X^i_{elite\_SF}$ is sailfish best position and $X^i_{injured\_s}$ is best position of sardines and X^i_{oldSF} is sailfish current position, $rand(0,1)$ is random number between 0, 1, λ_i as follows,

$$\lambda i = 2\lambda\, rand(0,1) \times PD - PD \quad (17)$$

The PD is a significant parameter for updating the sailfish position around prey school due to the number of prey is decreasing during the group hunting and the number of prey at each iteration as follows

$$PD = 1 - \left(\frac{N_{SF}}{N_{SF} + N_s} \right) \quad (18)$$

Where N_s and N_{SF} are number of sardines and sailfish at each iteration respectively. For imitating to update the sardines position at the ith iteration as follows,

$$X^{i}_{new\_s} = r \times \left(X^{i}_{elite\_SF} - X^{i}_{old\,s} + AP \right) \quad (19)$$

Where r denotes random number between 0,1 $X^{i}_{old\,s}$ is sardines current position $X^{i}_{elite\_SF}$ is sailfish best position and the total amount of sailfish power will saved in AP parameter, and it is generated as follows,

$$AP = A \times (1 - (2 \times Itr \times \varepsilon)) \quad (20)$$

Where A and ε are the value of power attack will be decreasing linearly from A to 0. In last the position of sailfish substitute for increase the hunting chance to new prey with the latest position of hunted sardines. They expressed as,

$$X^{i}_{SF} = X^{i}_{S}\ iff\ (si) < f(SFi) \quad (21)$$

Where, X^{i}_{S} and X^{i}_{SF} shows sardines and sailfish current position at ith iteration respectively.

3.4.1 Flowchart for SFO

The SFO and Gini index are select the optimum TSF parameters for each phase. This algorithm is tested using three torque signals and the appropriate mode select lowest phase value of the torque signal is automatically extract based on Gini index values. The result is indicate minimum value of torque ripple to compare with other two phase torque value. Therefore the SFO algorithm is tuned TSF parameters and permit minimum torque value for the SRM. Flowchart of SFO is given in figure 4.

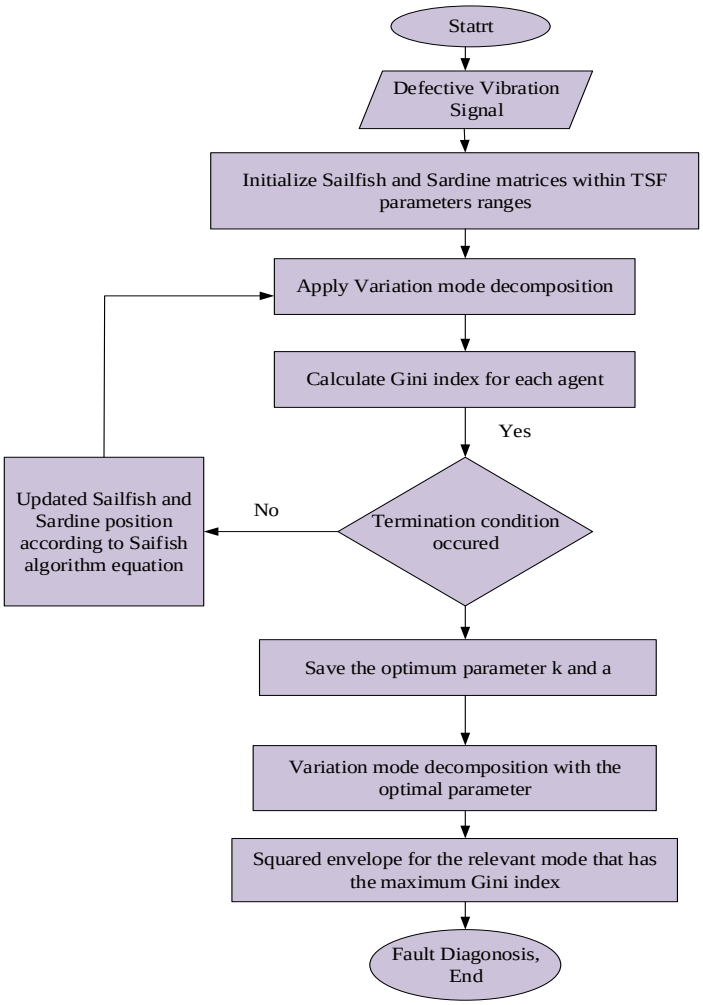

Figure 4: SFO Basic Flowchart

The Atom search Optimization (ASO) is used to optimize the position sensor in the proposed method. Each atom's position in the search space in ASO represents a solution that is based on its mass, with a better solution corresponding to a heavier mass and vice versa. Therefore, ASO optimize position sensor for control the rotor position of the SRM.

3.5 Atom Search Optimization (ASO)

Atom Search Optimization (ASO), an optimization approach motivated by molecular dynamics, and each atom's position in the search space symbolises a solution in the ASO method, where a better solution corresponds to a heavier mass and vice versa. According to their distance from one another, all of the atoms in the population will either attract or repel one another, which will cause the lighter atoms to gravitate towards the heavier ones [31]. When heavier atoms accelerate more slowly, they search more actively in local spaces for better solutions. Lighter atoms move more quickly, which forces them to scour the entire search space for new promising places.

The general optimization problems can be defined as

$$Minimize\ f(x),\ x=\left(x^1,....x^D\right) \tag{22}$$

For

$$Lb \le x \le Ub, Lb=\left[lb^1,....lb^D\right], Ub=\left[ub^1,.....ub^D\right] \tag{23}$$

Where, $x^d\left(d=1,....D\right)$ is denoted dth component of search space, lb^D is lower limit, and ub^D is upper limit for dth component. D denotes search space dimension.

Consider an atom population that has N atoms in order to solve this unconstrained optimization. The position of the ith atom is expressed by

$$x_i=\left[x_i^1,...x_i^D\right] \quad i=1,.....N \tag{24}$$

Where, $x_i^d\ \left(d=1,....D\right)$ denotes position component of the ith atom in a D-dimension.

Each atom dependent on others by the attraction among them, in the iteration of ASO. The repulsion can avoid the over concentration of atoms and the convergence of the algorithm, therefore increasing the exploration ability in the entire search space. The repulsion is gently weakens and the attraction gently strengthens, which signifies that the exploitation increases and exploration decreases. Each atom interacts with others by the attraction which ensures that the algorithm has a good exploitation capability.

3.5.1 Flowchart for ASO

In this proposed method ASO algorithm is used to select the correct rotor position for the SRM. The ASO is tune a position sensor in the motor. Basically ASO is select the better solution for the given parameters, therefore evaluate the each position, and sensing the correct position of the SRM. Flowchart for ASO is given in figure 5.

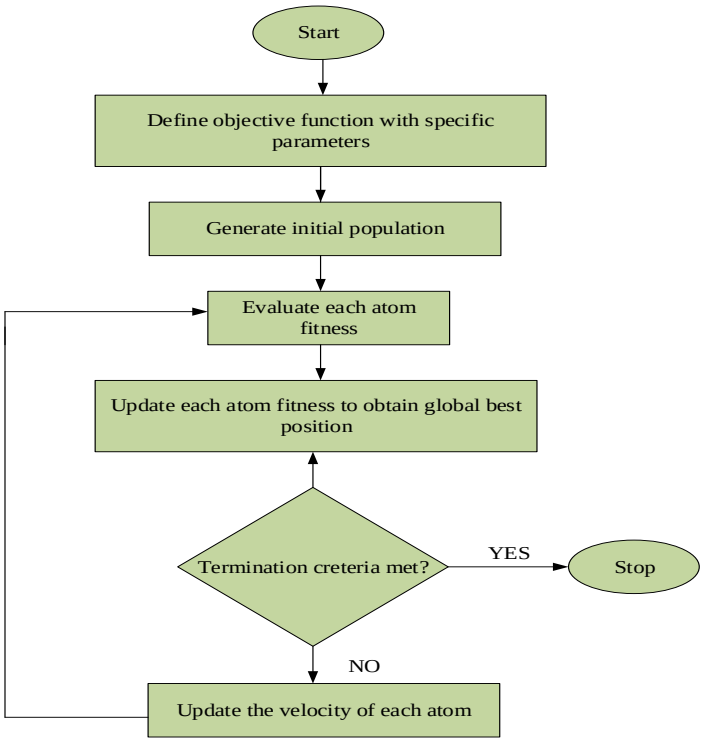

Figure 5: Basic Flowchart for ASO

4. Result and Discussion

The obtained result from the proposed, minimize the torque ripple and control the rotor position on Switched reluctance Motor (SRM) using predictive controllers is discussed here. The combined SFO-MPTC based TSF control strategies are reduce the torque ripple and using Atom Search Optimization (ASO) optimized rotor position in the proposed model.

Table 2: **Specification of SRM**

Stator Rotor Poles	8/6
Rated Power (kW)	15
Speed range (r/min)	100-1500
Stator Resistance (Ω)	1.7
Rated Torque $\left(N.m \right)$	95.5
Rated Current (A)	31

The proposed methodology of reduce the torque ripple and control the rotor position for SRM based on MPTC controller using SFO algorithm shows more effective result in analysed by utilizing the parameters. The proposed study is performed using Simulink and we used 15 kW SRM and 8/6 stator poles motor. The machine ratings are given in table 2. The Simulink model for the proposed MPTC based SRM with the SFO optimization algorithm is shown in figure 6. The speed, flux, current and torque are reveals from the proposed methodology.

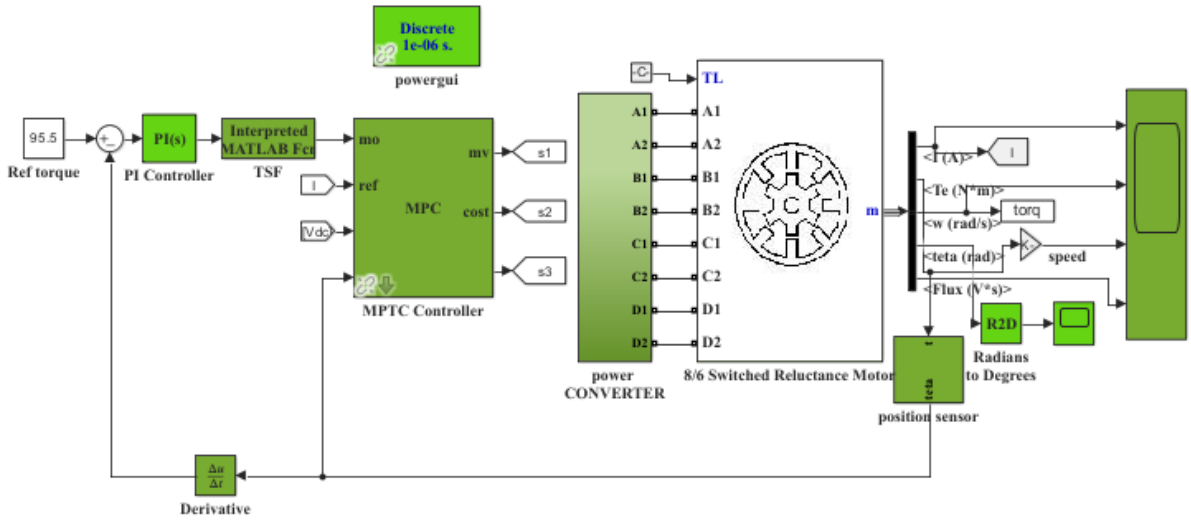

Figure 6: Simulink model diagram of MPTC based SRM system

The sample of reference torque waveforms for linear TSF of three phase SRM for T_{ref} =95.5 $N.m$ are shown in figure 7 (a). The corresponding reference current waveforms calculated using inverse $i(T,\theta)$ LUT are depicted in Figure (b). The current controller is then provided these current waveforms so it can track them.

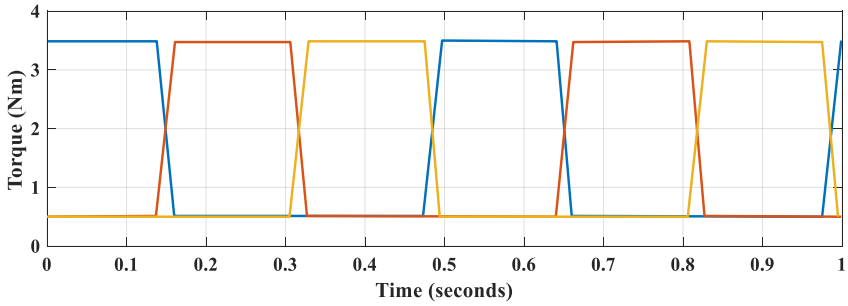

(a)

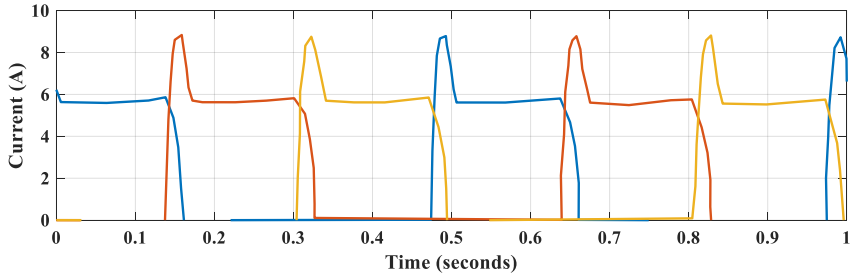

(b)

Figure 7: Reference phase torques and phase currents of the three-phase SRM using linear torque sharing function (TSF) (a) phase torques, and (b) phase currents.

Case 1: The simulated performance of the test SRM with linear TSF at 900 r/min under load torque of 95.5 N.m is presented in Figure 8 (a), and (b) is rotor position waveform of the SRM. Note that the turn on angle (θon) and the overlapping angle (θov) are set to 40° and 15° mechanical, respectively. We achieved the 19.5 N.m value of torque ripple. The response for the motor current, flux, and speed with respect to the time t=0.1 sec.

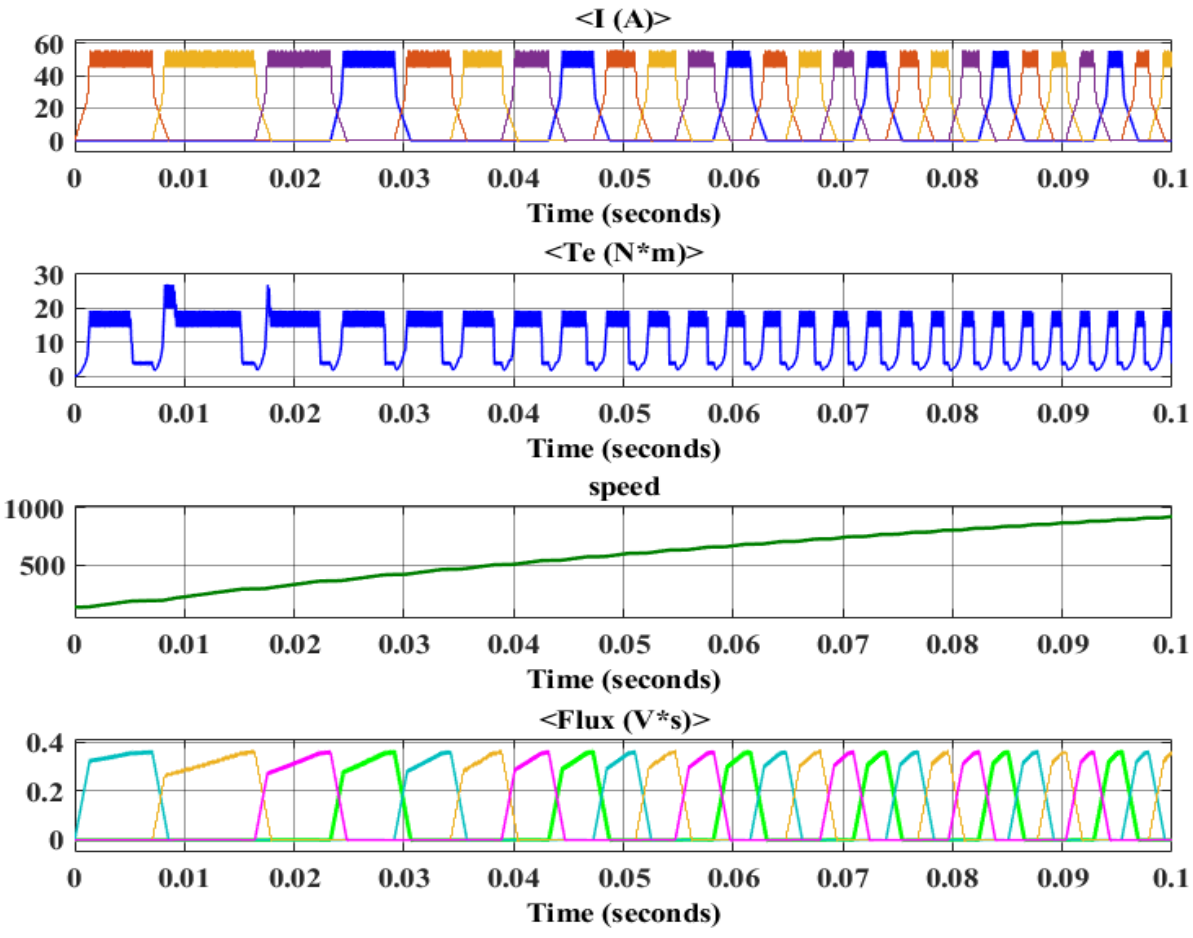

(a)

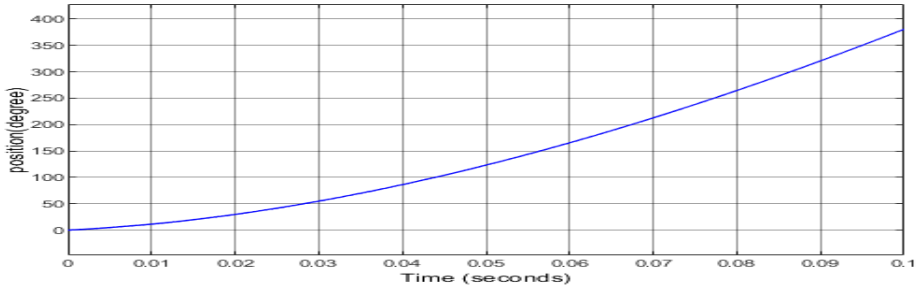

(b)

Figure 8: Current, speed, flux and torque waveforms, (b) Position waveform of the test SRM at 900 r/min (Linear TSF, $T_{ref} = 95.5\,N.m$ θ_{on} =40°, θ_{ov} =15°)

Case 2: The same simulation is repeated at a higher speed of 1100 r/min (Linear TSF, $T_{ref} = 95.5N.m$ $\theta_{on} = 40^{\circ}, \theta_{ov} = 15^{\circ}$.The waveforms of current, flux, speed and torque are shown in Figure 9 (a), and (b) shows rotor position waveform for the SRM.

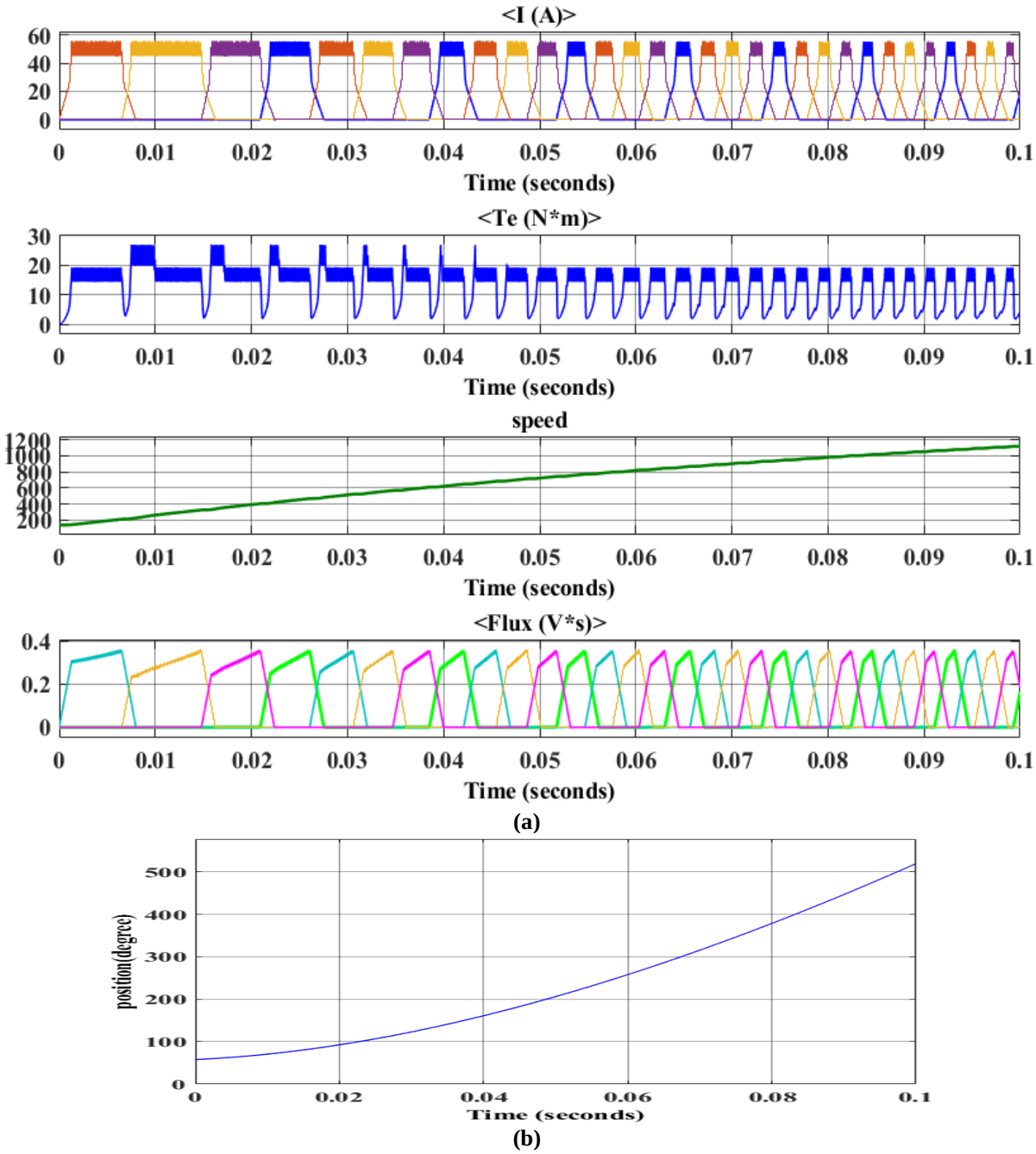

Figure 9: (a) Current, speed, flux, and torque waveforms (b) position waveform of the test SRM at 1100 r/min (Linear TSF, $T_{ref} = 95.5N.m, \theta_{on} = 40^{\circ}, \theta_{ov} = 15^{\circ}$)

Case 3: The same simulation is repeated at a higher speed of 1200 r/min (Linear TSF, $T_{ref} = 95.5N.m$ $\theta_{on} = 40^{\circ}, \theta_{ov} = 15^{\circ}$.The waveforms of current, speed, flux and torque ripple are shown in Figure 10 (a), and (b) shows the rotor position waveform of the SRM.

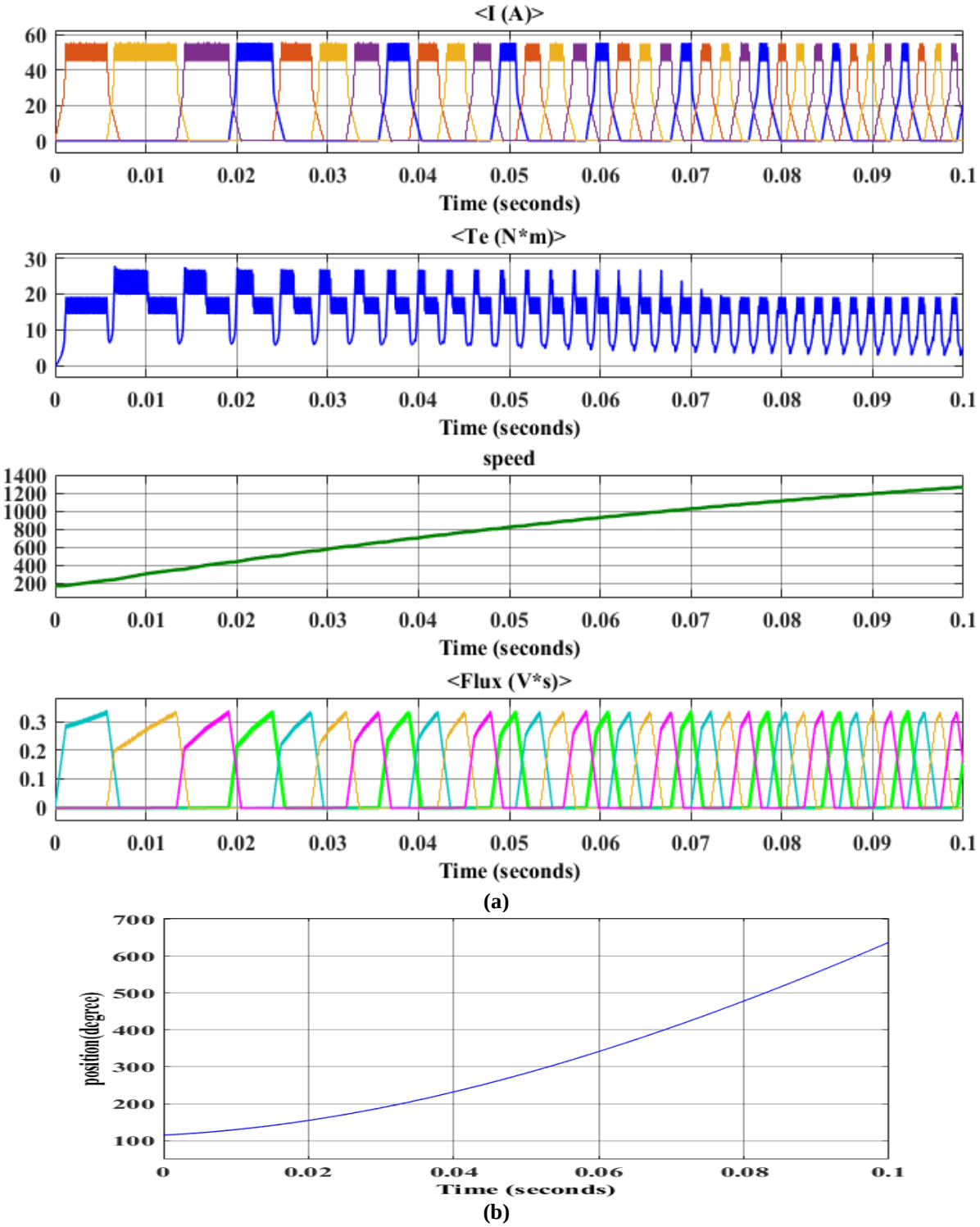

Figure 10: (a) Current, speed, flux, and torque waveforms (b) position waveform of the test SRM at 1200 r/min (Linear TSF, $T_{ref} = 95.5N.m$, $\theta_{on} = 40^\circ$ $\theta_{ov} = 15^\circ$)

Figures 9 and 10 shows that after the phase is turned off, the reference current tracking becomes worse at higher speeds, it results in the negative torque output and the current tail in the generating region and negative torque production. The SRM capacity to produce torque is highly limited close to the unaligned position, hence having a smaller turn-on angle results in a large reference current. As a result, employing the TSF to fire in advance is not possible. Therefore, at greater rotational speeds, TSF control technique cannot compete with traditional control methods. The reference current profiles are calculated offline in the current profiling procedure in order to meet the desired performance goals.

The SRM has torque characteristics and high nonlinear flux, so it makes more challenging to control compare with conventional AC drives. The predictive torque control is examine an acceptable technique to control SRM drive.

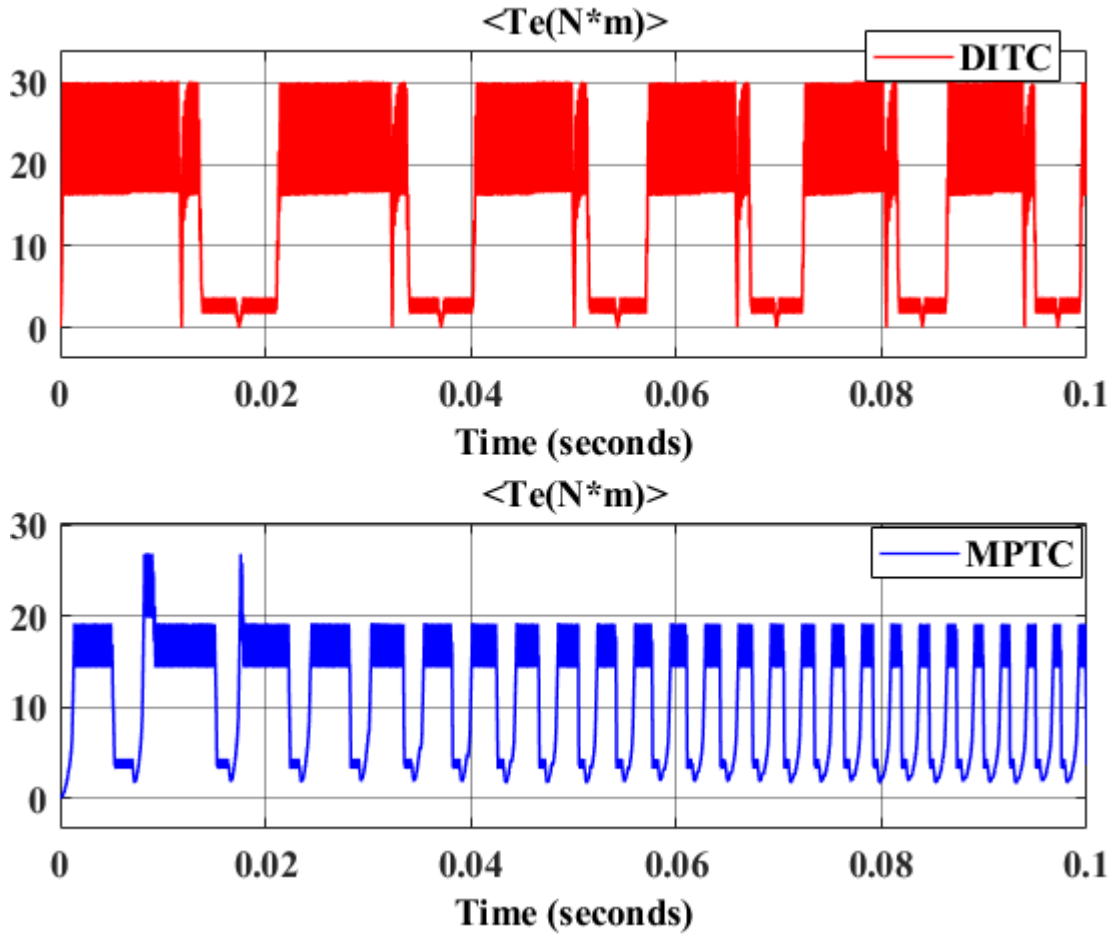

Figure 11: Comparison of torque ripple for SFO-MPTC and DITC

The dynamic characteristics of SFO-MPTC method, experiments are charge with the load torque vary from 95.5N.m with respect to the 900r/min speed and the result of proposed SFO-MPTC torque value is lower than existing DITC method. The result of torque ripple for proposed technique and DITC method are shown in figure 10. The torque ripple coefficient (T_{ripple}) of proposed SFO-MPTC is maintained at limited value, at different speed. Figure 10 shows the performance of SFO-MPTC and DITC at different speed with 95.5 $N.m$ load torque. The peak value of torque (T_{peak}) existing DITC is 2.57 $N.m$ and value of torque ripple (T_{ripple}) is 50.80%. In proposed SFO-MPTC, the peak value is 0.71 $N.m$, and the torque ripple is 19.5%.

5. Conclusion

In this proposed method, developed a technique named as MPTC based SFO algorithm using TSF function for minimize the torque ripple of SRM drive system. The theoretical analysis of the result will be following conclusion. The torque ripple can reduced by using torque sharing function, and this function is optimizing by the SFO. TSF has three torque values Ta, Tb, Tc, these values are evaluated in proposed MPTC method and select the minimum value of torque ripple to the SRM System. The Atom Search Optimization (ASO) can be used to optimize the position sensor. The position sensor is sensing correct rotor position of the SRM. And achieved the peak value of torque is 0.71 $N.m$, and the torque ripple is 19.5%. As demonstrated by the simulation test the proposed MPTC-SFO with TSF control strategy performs well to reduce the torque ripple and also control the rotor position more effectively to compare with the DITC method in SRM driving system .

Reference:

[1] Ren, Ping, Jingwei Zhu, Zhe Jing, Zhaoyan Guo, and Aide Xu. "Minimization of torque ripple in switched reluctance motor based on MPC and TSF." *IEEJ Transactions on Electrical and Electronic Engineering* 16, no. 11 (2021): 1535-1543.

[2] He, Xiaofeng, and Yao Yao. "An Improved Hybrid Control Scheme of a Switched Reluctance Motor for Torque Ripple Reduction." *Applied Sciences* 12, no. 23 (2022): 12283.

[3] A. Ahmed, Abdelsalam, Mahmoud M. Akl, and Essam Eddin M. Rashad. "A comparative dynamic analysis between model predictive torque control and field-oriented torque control of IM drives for electric vehicles." *International Transactions on Electrical Energy Systems* 31, no. 11 (2021): e13089.

[4] Bindal, Ranjit Kumar, and Inderderpreet Kaur. "Torque ripple reduction of induction motor using dynamic fuzzy prediction direct torque control." *ISA transactions* 99 (2020): 322-338.
[5] Aziz, Ahmed G. Mahmoud A., Hegazy Rez, and Ahmed A. Zaki Diab. "Robust Sensorless Model-Predictive Torque Flux Control for High-Performance Induction Motor Drives." *Mathematics* 9, no. 4 (2021): 403.
[6] Mohanraj, Deepak, Janaki Gopalakrishnan, Bharatiraja Chokkalingam, and Lucian Mihet-Popa. "Critical Aspects of Electric Motor Drive Controllers and Mitigation of Torque Ripple-Review." *IEEE Access* (2022).
[7] Yao, Xuliang, Jicheng Zhao, Jingfang Wang, Shengqi Huang, and Yishu Jiang. "Commutation torque ripple reduction for brushless dc motor based on an auxiliary step-up circuit." *IEEE access* 7 (2019): 138721-138731.Related worksRen, Ping, Jingwei Zhu, Zhe Jing, Zhaoyan Guo, and Aide Xu. "Minimization of torque ripple in switched reluctance motor based on MPC and TSF." *IEEJ Transactions on Electrical and Electronic Engineering* 16, no. 11 (2021): 1535-1543.
[8] Al-Amyal, Fahad, László Számel, and Mahmoud Hamouda. "An enhanced direct instantaneous torque control of switched reluctance motor drives using ant colony optimization." *Ain Shams Engineering Journal* 14, no. 5 (2023): 101967.
[9] Li, Cunhe, Qinjun Du, and Xing Liu. "Indirect predictive torque control for switched reluctance motor in EV application." *Energy Reports* 8 (2022): 857-865.
[10] Sun, Xiaodong, Jiangling Wu, Gang Lei, Youguang Guo, and Jianguo Zhu. "Torque ripple reduction of SRM drive using improved direct torque control with sliding mode controller and observer." *IEEE Transactions on Industrial Electronics* 68, no. 10 (2020): 9334-9345.
[11] Reddy, P. Krishna, Deepak Ronanki, and P. Parthiban. "Direct torque and flux control of switched reluctance motor with enhanced torque per ampere ratio and torque ripple reduction." *Electronics Letters* 55, no. 8 (2019): 477-478.
[12] Wang, Shuanghong, Zihui Hu, and Xiupeng Cui. "Research on novel direct instantaneous torque control strategy for switched reluctance motor." *IEEE Access* 8 (2020): 66910-66916.
[13] Hamouda, Mahmoud, Amir Abdel Menaem, Hegazy Rezk, Mohamed N. Ibrahim, and László Számel. "Comparative evaluation for an improved direct instantaneous torque control strategy of switched reluctance motor drives for electric vehicles." *Mathematics* 9, no. 4 (2021): 302.
[14] Al-Amyal, Fahad, Mahmoud Hamouda, and Laszlo Szamel. "Performance improvement based on adaptive commutation strategy for switched reluctance motors using direct torque control." *Alexandria Engineering Journal* 61, no. 11 (2022): 9219-9233.
[15] Cheng, Yong. "Modified PWM direct instantaneous torque control system for SRM." *Mathematical Problems in Engineering* 2021 (2021): 1-13.
[16] De Paula, Marcelo Vinicius, and Tárcio André dos Santos Barros. "A sliding mode DITC cruise control for SRM with steepest descent minimum torque ripple point tracking." *IEEE Transactions on Industrial Electronics* 69, no. 1 (2021): 151-159.
[17] Jing, Benqin, Xuanju Dang, Zheng Liu, and Shike Long. "Torque ripple suppression of switched reluctance motor based on fuzzy indirect instant torque control." *IEEE Access* 10 (2022): 75472-75481.
[18] Bogusz, Piotr, Mariusz Korkosz, Jan Prokop, and Mateusz Daraż. "Analysis Performance of SRM Based on the Novel Dependent Torque Control Method." *Energies* 14, no. 24 (2021): 8203.
[19] Dang, Xuanju, Yazhou Shi, and Huimin Peng. "Torque–flux linkage recurrent neural network adaptive inversion control of torque for switched reluctance motor." *IET Electric Power Applications* 14, no. 9 (2020): 1612-1623.
[20] Fang, Gaoliang, Filipe P. Scalcon, Dianxun Xiao, Rodrigo P. Vieira, Hilton A. Gründling, and Ali Emadi. "Advanced control of switched reluctance motors (SRMs): A review on current regulation, torque control and vibration suppression." *IEEE Open Journal of the Industrial Electronics Society* 2 (2021): 280-301.
[21] Ren, Ping, Jingwei Zhu, Zhe Jing, Zhaoyan Guo, and Aide Xu. "Minimization of torque ripple in switched reluctance motor based on MPC and TSF." *IEEJ Transactions on Electrical and Electronic Engineering* 16, no. 11 (2021): 1535-1543.
[22] Kimpara, Marcio LM, Renata RC Reis, Luiz EB Da Silva, Joao OP Pinto, and Babak Fahimi. "A two-step control approach for torque ripple and vibration reduction in switched reluctance motor drives." *IEEE Access* 10 (2022): 82106-82118.
[23] Al-Amyal, Fahad, László Számel, and Mahmoud Hamouda. "An enhanced direct instantaneous torque control of switched reluctance motor drives using ant colony optimization." *Ain Shams Engineering Journal* 14, no. 5 (2023): 101967.
[24] Chenchireddy, Kalagotla, V. Kumar, G. Eswaraiah, Khammampati R. Sreejyothi, Shabbier Ahmed Sydu, and Lukka Bhanu Ganesh. "Torque Ripple Minimization in Switched Reluctance Motor by Using Artificial Neural Network." In *2022 IEEE 2nd International Conference on Sustainable Energy and Future Electric Transportation (SeFeT)*, pp. 1-6. IEEE, 2022.
[25] Jing, Benqin, Xuanju Dang, Zheng Liu, and Shike Long. "Torque ripple suppression of switched reluctance motor based on fuzzy indirect instant torque control." *IEEE Access* 10 (2022): 75472-75481.
[26] Chen, Tong, and Guoyang Cheng. "Comparative Investigation of Torque-ripple Suppression Control Strategies Based on Torque-sharing Function for Switched Reluctance Motor." *CES Transactions on Electrical Machines and Systems* 6, no. 2 (2022): 170-178.

[27] Seshadri, Arjun, Natesan C. Lenin, Sanjeevikumar Padmanaban, and Baseem Khan. "Impact of stator slot geometry on the windage loss in a high-speed linear switched reluctance motor." *IET Electric Power Applications* 16, no. 4 (2022): 447-462.
[28] Gong, Chao, Yihua Hu, Mingyao Ma, Jinqiu Gao, and Ke Shen. "Novel analytical weighting factor tuning strategy based on state normalization and variable sensitivity balance for PMSM FCS-MPTC." *IEEE/ASME Transactions on Mechatronics* 25, no. 3 (2020): 1690-1694.
[29] Arroyo, Javier, Carlo Manna, Fred Spiessens, and Lieve Helsen. "Reinforced model predictive control (RL-MPC) for building energy management." *Applied Energy* 309 (2022): 118346.
[30] Naji, Hamid Reza, Soodeh Shadravan, Hossien Mousa Jafarabadi, and Hossien Momeni. "Accelerating sailfish optimization applied to unconstrained optimization problems on graphical processing unit." *Engineering Science and Technology, an International Journal* 32 (2022): 101077.
[31] Junsittiwate, Rawinun, Thongchai Rohitatisha Srinophakun, and Somboon Sukpancharoen. "Multi-objective atom search optimization of biodiesel production from palm empty fruit bunch pyrolysis." *Heliyon* 8, no. 4 (2022): e09280.